Solving the P-O/P-OH Riddle: Direct Synthesis and Neutron Diffraction Characterization of Dianionic Dithiophosphonates

Michael N. Pillay,[a] Min-Chi Li,[a] Yu-Rong Ni,[a] Wei-Jung Yen,[a] Tzu-Hao Chiu,[a] Xiaoping Wang,[b] Jean-Yves Saillard [c] and C. W. Liu[a]*

[a] Department of Chemistry, National Dong Hwa University, No. 1, Sec. 2, Da Hsueh Rd., Hualien 97401, Taiwan. Email: chenwei@gms.ndhu.edu.tw
[b] Neutron Scattering Division Neutron Sciences Directorate, Oak Ridge National Laboratory, Oak Ridge, Tennessee 37831, USA.
[c] Univ Rennes, CNRS, ISCR-UMR 6226, Rennes 35000, France.

Supporting information

Experimental

All commercial reagents are sourced as follows: nickel(II) chloride hexahydrate (STREM chemicals, 99+%); tetrabutylammonium chloride (ACROS chemicals, 95%); phosphorus pentasulfide(Sigma-Aldrich, 99%); anisole (Sigma-Aldrich, 99%). Lawesson's reagent was prepared according to literature procedures.[S1] NMR spectra were recorded on a Bruker Advance 400 MHz spectrometer, operating at 400 MHz for ^{1}H and 161.97 MHz for ^{31}P{^{1}H}. ESI-MS and ESI-TOF-MS spectra were recorded on an AB SCIE X QSTAR® XL High-Resolution Electrospray Mass spectrometer and a Fison Quattro Bio-Q (Fisons Instruments, VG Biotech, UK).

Single crystal X-ray diffraction data were collected using an XtaLAB Synergy, single-source at home/near, HyPix-Arc 100 diffractometer operating at T = 100.01(10) K. Data were measured using w scans of 0.5° per frame for 0.1 s using Cu K_a radiation. The diffraction pattern was indexed, and the total number of runs and images was determined based on the strategy calculation from the CrysAlisPro program (Rigaku). The total number of runs and images was based on the strategy calculation from the CrysAlisPro program (Rigaku), and the unit cell was refined using CrysAlisPro (Rigaku, Version 1.171.44.120a, 2025). Data reduction, scaling, and absorption corrections were performed using CrysAlisPro (Rigaku, V1.171.44.120a, 2025). The structure was solved with the ShelXT (Sheldrick, 2015) structure solution program using the Intrinsic Phasing solution method and by using Olex2 as the graphical interface.[S2,S3] Further details provided in Table S2-4.

Single-crystal neutron diffraction was recorded on a TOPAZ single-crystal neutron time-of-flight (TOF) Laue diffractometer at ORNL's Spallation Neutron Source.[S4] A purple, block-shaped crystal was attached to a MiTeGen loop using a perfluorinated grease (Krytox GPL 205) and transferred to the TOPAZ goniometer for data collection at 100 K. Crystal orientations were optimized with CrystalPlan software,[S5] to ensure better than 95% coverage of a hemisphere of reciprocal space. Raw peak intensities were obtained using the 3-D ellipsoidal Q-space integration method available in Mantid.[S6] Data normalization, including Lorentz, neutron 6 TOF spectrum, and detector efficiency corrections, was carried out with the ANVRED3 program.[S7] The reduced data were saved in SHELX HKLF2 format, in which the neutron wavelength for each reflection was recorded separately. Further details provided in Table S5.

Geometry optimizations were carried out within the formalism of the density functional theory (DFT) with the Gaussian 16 package,[S8] using the BP86 functional[S9,S10] and the Def2-TZVP basis set from EMSL Basis Set Exchange Library.[S11,S12]

Table S1. Comparison of computational and X-ray parameters.

	***syn*-[Ni(L_{PO})$_2$]**	***anti*-[Ni(L_{PO})$_2$]**	***syn*-[Pd(L_{PO})$_2$]**	***anti*-[Pd(L_{PO})$_2$]**	**[(PPh_3)Pt(L_{PO})$_2$],**
PO bond length (Å) (x-ray)	1.509(1) 1.513(1) (neutron)	1.528(3)	1.509(2)	-	1.491(2)
PO bond length (Å) (DFT)	1.512	1.511	1.511	1.510	1.496
ΔE (kcal/mol)	0.86	0	0.65	0	-
ΔG (kcal/mol)	0.86	0	0.65	0	-

Synthesis of $(NH_4)_2[S_2P(O)(C_6H_4OMe)]$, $(NH_4)_2[L_{PO}]$.

A Schlenk flask was charged with Lawesson's reagent (2.063 g, 5.10mmol) and suspended in THF. To the suspension, two molar equivalents of Di-H2O (185 µL, 10.20 mmol) were added, and the mixture was sonicated for 5 min, or until no visible suspension remained. Ammonia

gas (NH_3) was then bubbled through the solution, resulting in the immediate formation of a white precipitate. The solvent was removed in vacuo, and the powder consolidated with ether to yield a white salt. (Yield 2.384 g, 92 %) ^{1}H NMR (D_2O): δ (ppm), *J*(Hz), 3.88(s, OCH_3, 3H), 7.00 (dd, ArCH, 2H, *J* = 2.12, 8.82 Hz), 7.92 (dd, ArCH, 2H, *J* = 8.53, 12.81) ^{31}P NMR (D_2O): δ (ppm), 73.60.

Synthesis of $(NH_4)_2[Ni(L_{PO})_2]$, (1).

To a Schlenk flask containing an aqueous solution of $(NH_4)_2$[**L_{PO}**] (200 mg, 0.786 mmol), $NiCl_2{\cdot}6H_2O$ (93 mg, 0.393 mmol) was added, resulting in the instantaneous formation of a purple solution. The solution is allowed to stir for 10 min, after which the solvent is removed in vacuo to yield a pale purple powder. The powder is dissolved in deionized H_2O and allowed to evaporate, yielding purple crystals, which are then collected by filtration. (Yield 0.118 g, 57 %). ^{1}H NMR (400 MHz, D_2O): δ (ppm), *J*(Hz), 3.85(s, OCH_3, 6H), 6.96 (d, ArCH, 2H, *J* = 7.85), 8.31 (dd, ArCH, 2H, *J* = 8.55, 12.15). ^{31}P-NMR (161.97 MHz, D_2O): δ (ppm), 72.28. ESI-MS (m/z) (cal.) 496.8848(496.8839) for ([Ni{($S_2P(O)(1,4\text{-}C_6H_4OMe)$}$_2$] + $3H^+$).

Synthesis of $(NBu_4)_2[Ni(L_{PO})_2]$, (1_{TBA}).

A solution of **1** (100 mg, 0.188 mmol) was subjected to ion-pair extraction within a biphasic DCM/H_2O (1:1) system. Upon the addition of tetrabutylammonium chloride $N(But)_4Cl$ (105 mg, 0.376 mmol), the mixture was stirred for 10 min. The resulting ion-exchange reaction formed the lipophilic ion-pair **1TBA**, evidenced by the rapid transfer of the characteristic purple color from the hydrophilic upper aqueous layer to the lipophilic lower dichloromethane (DCM) layer. The organic phase was subsequently separated, dried over anhydrous magnesium sulfate, and filtered. Slow solvent evaporation of the filtrate yielded crystalline **1TBA**. (Yield 310 mg, 84 %) ^{1}H-NMR (400 MHz, $CDCl_3$): δ (ppm), *J*(Hz), 0.93 (t, CH_3, 4H, *J* = 7.3), 1.39 (m, CH_2, 16H), 1.59 (m, CH_2, 16H),2.60 (s, OCH_3, 6H), 3.29 (t, CH_2, 16H, *J* = 8.4), 6.79 (dd, 4H, *J* = 8.7, 2.0),8.30 (d, 4H, *J* = 9.5). ^{31}P-NMR (161.97 MHz, $CDCl_3$): δ (ppm), 62.88.

Synthesis of $(NH_4)_2[Pd(L_{PO})_2]$, (2).

To a Schlenk flask containing an aqueous solution of $(NH_4)_2$[**L_{PO}**] (200 mg, 0.786 mmol), [$Pd(O_2CCH_3)_2$](88mg, 0.393 mmol) was added, resulting in the instantaneous formation of a

dark brown solution. The solution is allowed to stir for 10 min, after which the solvent is removed in vacuo to yield a pale purple powder. The powder is dissolved in deionized H_2O and allowed to evaporate, yielding purple crystals, which are then collected by filtration. (Yield 0.118 g, 57 %). [Note: The *syn* and *anti*-conformations are observed in solution NMR for the aromatic ^{1}H and ^{31}P nuclei, in a ratio of 3:1 (anti:syn)] ^{1}H NMR (400 MHz, D_2O): δ (ppm), *J*(Hz), 3.81(s, OCH_3, 6H), *anti*: [6.96 (d, ArCH, 2H, *J* = 8.82, 2.22), 7.97 (dd, ArCH, 2H, *J* = 8.91, 13.01)]; *syn*: [7.01 (d, ArCH, 2H, *J* = 8.77, 2.22), 8.01 (dd, ArCH, 2H, *J* = 7.9, 12.32)];. ^{31}P-NMR (161.97 MHz, D_2O): δ (ppm), 75.81(s), 76.63(s)

Synthesis of [$(PPh_3)_2Pt(L_{PO})$], (3).

To a Schlenk flask containing $(NH_4)_2$[**L_{PO}**] (12 mg, 0.05 mmol) dissolved in DI-H_2O, a DCM solution of [*cis*-$(PPh_3)PtCl_2$](39 mg, 0.05 mmol) was added. The solution was allowed to stir for 10 min, after which the solvent was removed in vacuo to yield a pale-yellow powder. The powder is redissolved in DCM, filtered through celite, and allowed to evaporate, yielding pale yellow crystals. (Yield 34 mg, 74 %). ^{1}H NMR (400 MHz, $(CD_3)_2CO$): δ (ppm), *J*(Hz), 3.83(s, OCH_3, 3H), 6.87 (d, ArCH(L_{PO}), 2H, *J* = 8.8, 2.6), 7.16 (m, ArCH(PPh_3)), 7.39 (m, ArCH(L_{PO}),7.97 (dd, ArCH(L_{PO}), 2H, *J* = 8.8, 12.7);. ^{31}P-NMR (161.97 MHz, $(CD_3)_2CO$): δ (ppm), *J*(Hz), 18.6 ppm (t, P_{LPO}, $J_{P\text{-}P}$ = 4.7 Hz), 58.4 ppm (d, P_{PPh3}, $J_{P\text{-}P}$ = 4.7; ^{31}P-^{195}Pt satellites: $J_{Pt\text{-}P}$ = 4050)

Table S2. SCXRD details and parameters for $\mathbf{L_{PO}}$, **1** and **1TBA**.

Compound	$\mathbf{L_{PO}}$	**1**	**1TBA**
CCDC #	2501518	2501519	2501520
Chemical formula	$C_{14}H_{32}N_4O_5P_2S_4$	$C_{14}H_{14}O_4P_2NiS_4{\cdot}H_2O{\cdot}2(H_4N)$	$2(C_7H_7Ni_{0.5}O_2PS_2){\cdot}C_{16}H_{36}N$
***M*$_r$**	526.61	549.24	737.60
Crystal system, space group	Monoclinic, $P2_1/c$	Monoclinic, $P2_1/c$	Monoclinic, $C2/c$
Temperature (K)	100	293	100
***a*, *b*, *c* (Å)**	12.1011 (2), 10.9171 (2), 9.2190 (1)	16.4408 (3), 10.4823 (2), 14.5603 (3)	36.3137 (10), 9.4106 (2), 22.9791 (6)
β (°)	97.586 (2)	112.818 (2)	111.905 (3)
***V* (Å^3)**	1207.25 (3)	2312.91 (8)	7285.8 (3)
Z	2	4	8
m (mm^{-1})	5.16	6.15	4.01
Crystal size (mm)	0.15 × 0.13 × 0.11	0.15 × 0.08 × 0.03	0.24 × 0.14 × 0.09
	Data collection		
Absorption correction	Gaussian *CrysAlis PRO* 1.171.44.120a (Rigaku Oxford Diffraction, 2025). Numerical absorption correction based on Gaussian integration over a multifaceted crystal model. Empirical absorption correction using spherical harmonics, implemented in SCALE3 ABSPACK scaling algorithm.		
***T*$_{min}$, *T*$_{max}$**	0.756, 0.973	0.352, 0.825	0.604, 1.000
No. of measured, independent and observed [*I* > 2σ(*I*)] reflections	46159, 2489, 2443	14427, 4312, 3882	37450, 7409, 5880
***R*$_{int}$**	0.047	0.019	0.074
(sin θ/λ)$_{max}$ (Å^{-1})	0.632	0.634	0.634
	Refinement		
R*[*F*^{2} > 2σ(*F*^{2})], *wR*(*F*^{2}), *S	0.033, 0.088, 1.08	0.024, 0.066, 1.08	0.062, 0.179, 1.07
No. of reflections	2489	4594	7409
No. of parameters	172	295	453
No. of restraints	0	0	237
H-atom treatment	mixture of independent and constrained refinement	mixture of independent and constrained refinement	H-atom parameters constrained
	$w = 1/[\sigma^2(F_o^2) + (0.0438P)^2 + 1.4527P]$ where $P = (F_o^2 + 2F_c^2)/3$	$w = 1/[\sigma^2(F_o^2) + (0.0335P)^2 + 0.5178P]$ where $P = (F_o^2 + 2F_c^2)/3$	$w = 1/[\sigma^2(F_o^2) + (0.0965P)^2 + 11.7095P]$ where $P = (F_o^2 + 2F_c^2)/3$
Δρ$_{max}$, Δρ$_{min}$ (e Å^{-3})	0.42, -0.39	0.25, -0.28	1.29, -0.46

Computer programs: *CrysAlis PRO* system (CCD 44.123a 64-bit (release 06-10-2025)), *CrysAlis PRO* 1.171.44.123a (Rigaku OD, 2025), *SHELXT* (Sheldrick, 2015), *SHELXL2019*/2 (Sheldrick, 2019), *SHELXL* 2019/3 (Sheldrick, 2015), Olex2 1.5-ac7-018 (Dolomanov *et al.*, 2009).

Table S3. SCXRD details and parameters for **2** and **3**.

Compound	**2**	**3**
CCDC #	2503642	2503643
Chemical formula	$C_{14}H_{14}O_4P_2PdS_4{\cdot}H_2O{\cdot}2(H_4N)$	$C_{44}H_{39}Cl_2O_2P_3PtS_2$
***M*$_r$**	596.93	1022.77
Crystal system, space group	Monoclinic, $P2_1/c$	Triclinic, $P\bar{1}$
Temperature (K)	293	100
Chemical formula	$C_{14}H_{14}O_4P_2PdS_4{\cdot}H_2O{\cdot}2(H_4N)$	$C_{44}H_{39}Cl_2O_2P_3PtS_2$
α,β,γ(°)	90, 112.913 (2), 90	77.314 (1), 87.495 (1), 76.672 (1)
***V* (Å^3)**	2342.34 (6)	2032.11 (4)
Z	4	2
m (mm^{-1})	Cu *K*α	Cu *K*α
Crystal size (mm)	0.25 × 0.16 × 0.1	0.16 × 0.09 × 0.05
	Data collection	
Absorption correction	Gaussian *CrysAlis PRO* 1.171.44.120a (Rigaku Oxford Diffraction, 2025). Numerical absorption correction based on Gaussian integration over a multifaceted crystal model. Empirical absorption correction using spherical harmonics, implemented in SCALE3 ABSPACK scaling algorithm.	
T_{min}, T_{max}	0.007, 0.154	0.608, 1.000
No. of measured, independent and observed [$I > 2\sigma(I)$] reflections	23412, 4782, 4470	78921, 8349, 8188
R_{int}	0.068	0.075
(sin θ/λ)$_{max}$ (Å^{-1})	0.634	0.634
	Refinement	
$R[F^2 > 2\sigma(F^2)]$, $wR(F^2)$, S	0.049, 0.130, 1.06	0.029, 0.076, 1.05
No. of reflections	4782	8349
No. of parameters	285	504
No. of restraints	0	3
H-atom treatment	H atoms treated by a mixture of independent and constrained refinement	H atoms treated by a mixture of independent and constrained refinement
	$w = 1/[\sigma^2(F_o^2) + (0.0946P)^2 + 0.0431P]$ where $P = (F_o^2 + 2F_c^2)/3$	$w = 1/[\sigma^2(F_o^2) + (0.0384P)^2 + 4.5885P]$ where $P = (F_o^2 + 2F_c^2)/3$
Δρ$_{max}$, Δρ$_{min}$ (e Å^{-3})	1.14, −1.08	1.02, −1.82

Computer programs: *CrysAlis PRO* system (CCD 44.123a 64-bit (release 06-10-2025)), *CrysAlis PRO* 1.171.44.123a (Rigaku OD, 2025), *SHELXT* (Sheldrick, 2015), *SHELXL2019*/2 (Sheldrick, 2019), *SHELXL* 2019/3 (Sheldrick, 2015), Olex2 1.5-ac7-018 (Dolomanov *et al.*, 2009).

Table S4. Single-crystal neutron diffraction details and parameters.

Compound	**1**
CCDC#	2501448
Chemical formula	$C_{14}H_{14}NiO_4P_2S_4 \cdot H_2O \cdot 2(H_4N)$
***M*$_r$**	549.24
Crystal system, space group	Monoclinic, $P2_1/c$
Temperature (K)	90
***a*, *b*, *c* (Å)**	16.3772 (3), 10.4693 (1), 14.2568 (2)
β (°)	112.281 (1)
***V* (Å^3)**	2261.93 (6)
Z	4
Radiation type	Neutron, λ = 1.00 Å
m (mm^{-1})	0.18
Crystal size (mm)	1.20 × 1.10 × 0.85
	Data collection
Diffractometer	TOPAZ
Absorption correction	For a sphere C. W. Dwiggins, Jr., Acta Cryst. A31, 395 (1975).
***T*$_{min}$, *T*$_{max}$**	0.704, 0.888
No. of measured, independent and observed [*I* > 2σ(*I*)] reflections	58323, 8404, 5967
***R*$_{int}$**	0.185
(sin θ/λ)$_{max}$ (Å^{-1})	0.979
	Refinement
R*[*F*^{2} > 2σ(*F*^{2})], *wR*(*F*^{2}), *S	0.047, 0.077, 1.10
No. of reflections	8404
No. of parameters	470
H-atom treatment	All H-atom parameters refined
Δρ$_{max}$, Δρ$_{min}$ (e Å^{-3})	0.85, -0.88

Computer programs: SNS EPICS, TOPAZ Mantid Python Program, *SHELXL2018*/3 (Sheldrick, 2018).

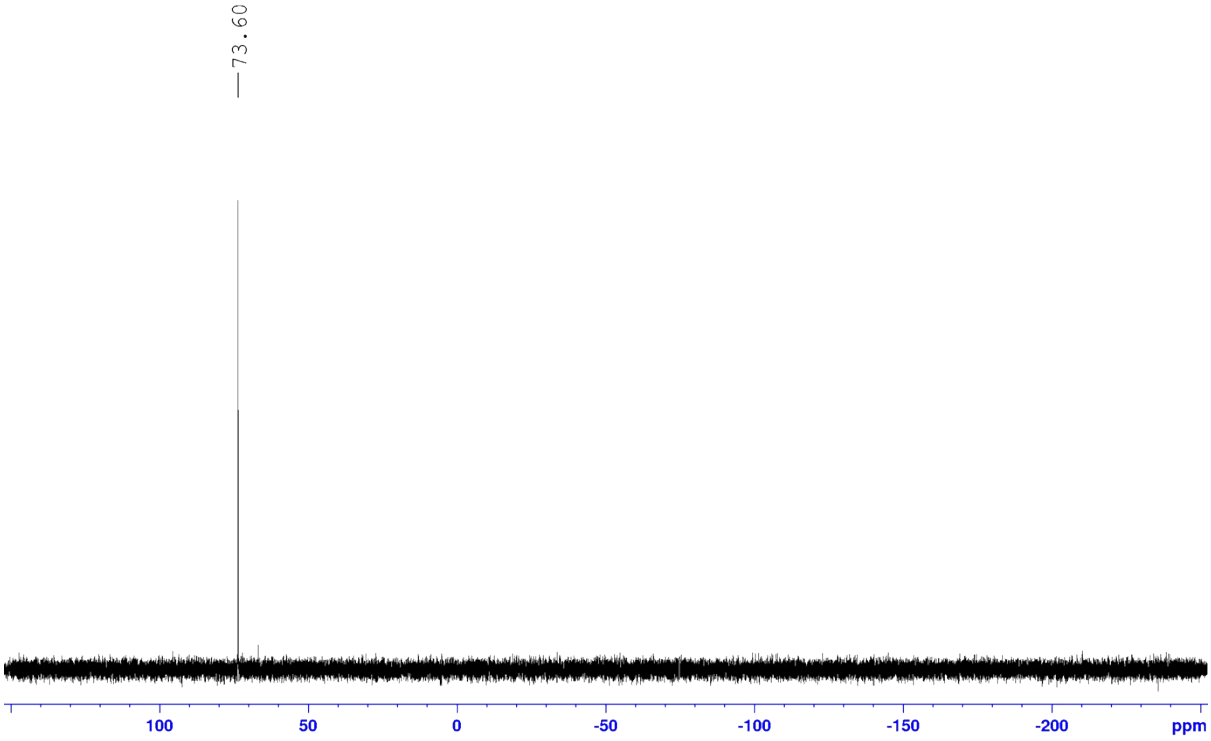

Figure S1. ^{31}P NMR of $\mathbf{L_{PO}}$ recorded in D_2O at room temperature.

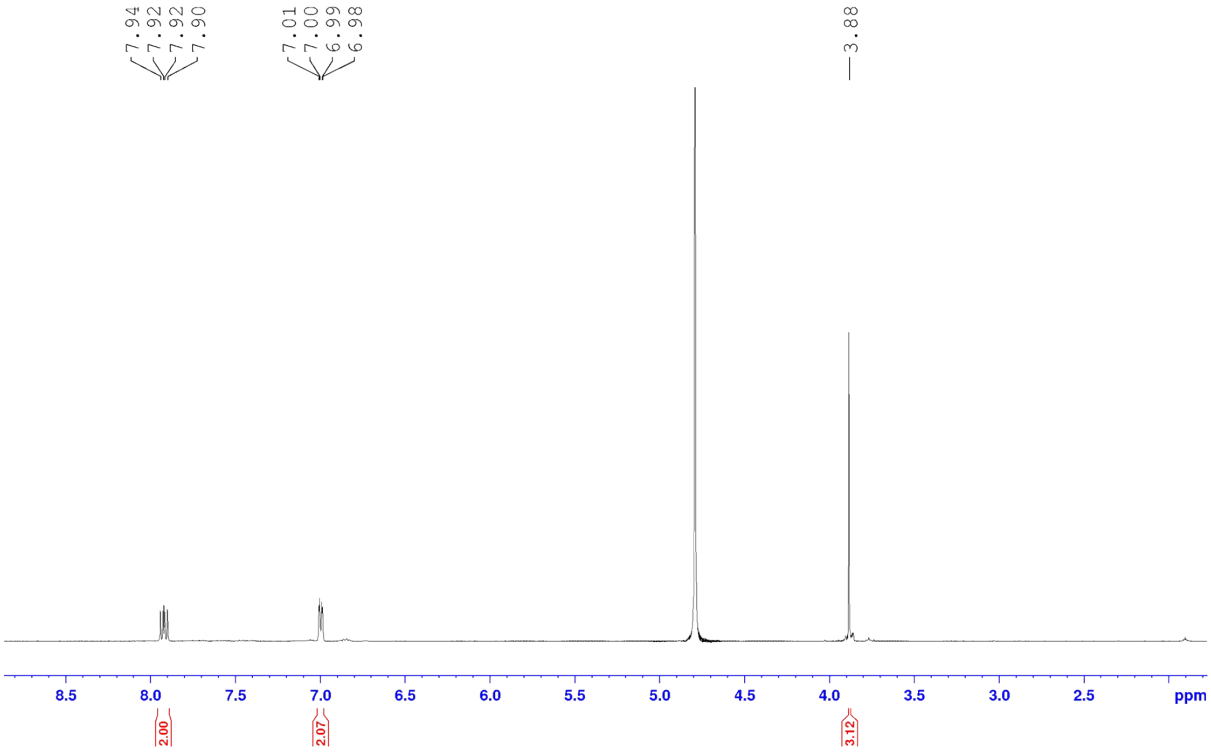

Figure S2. ^{1}H NMR of $\mathbf{L_{PO}}$ recorded in D_2O at room temperature.

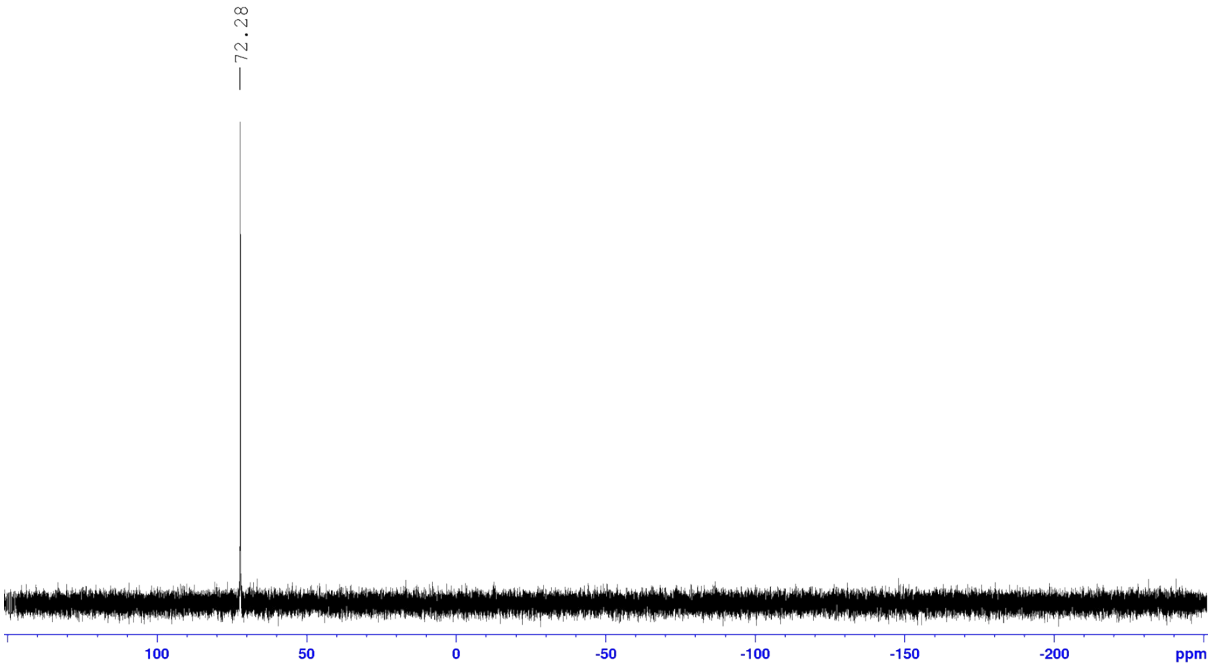

Figure S3. ^{31}P NMR of $(NH_4)_2[Ni(L_{PO})_2]$ recorded in D_2O at room temperature.

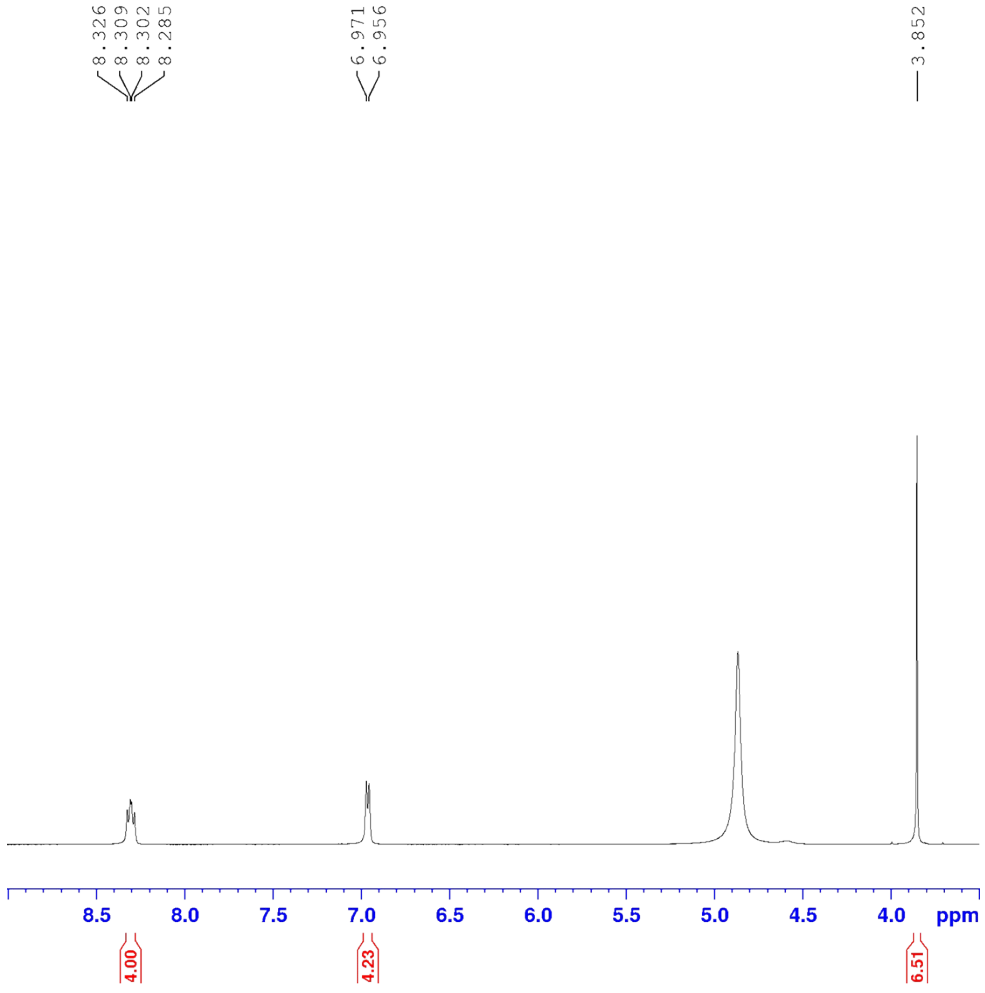

Figure S4. ^{1}H NMR of $(NH_4)_2[Ni(L_{PO})_2]$ recorded in D_2O at room temperature.

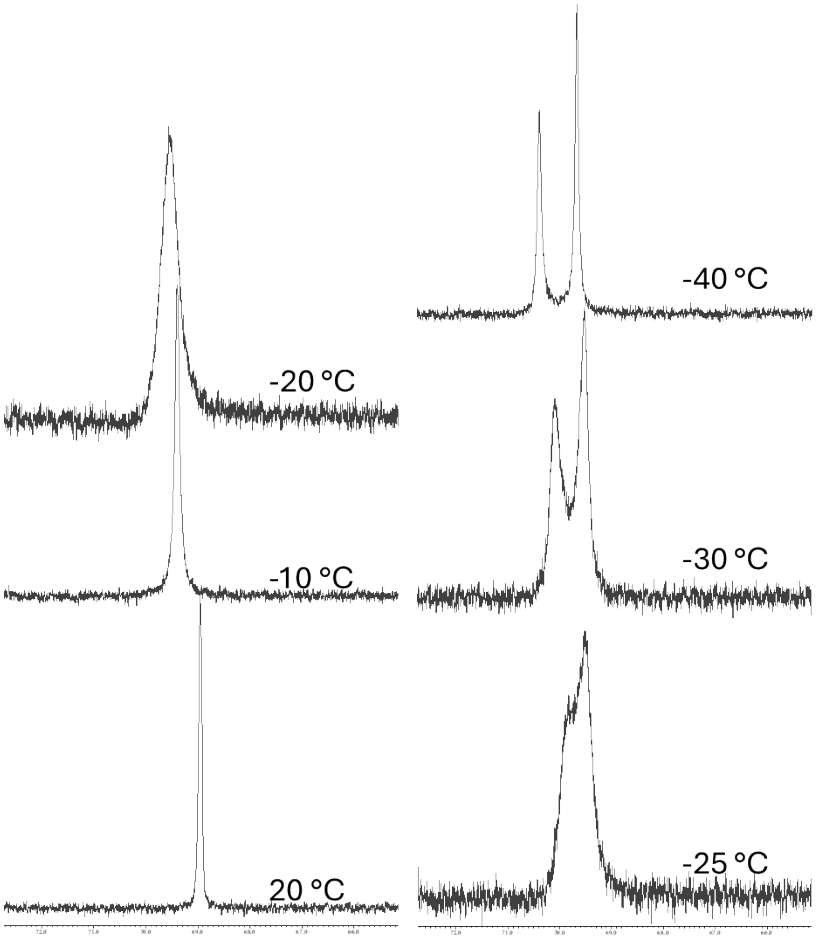

Figure S5. Variable temperature ^{31}P NMR of $(NH_4)_2[Ni(L_{PO})_2]$ recorded in CD_3OD.

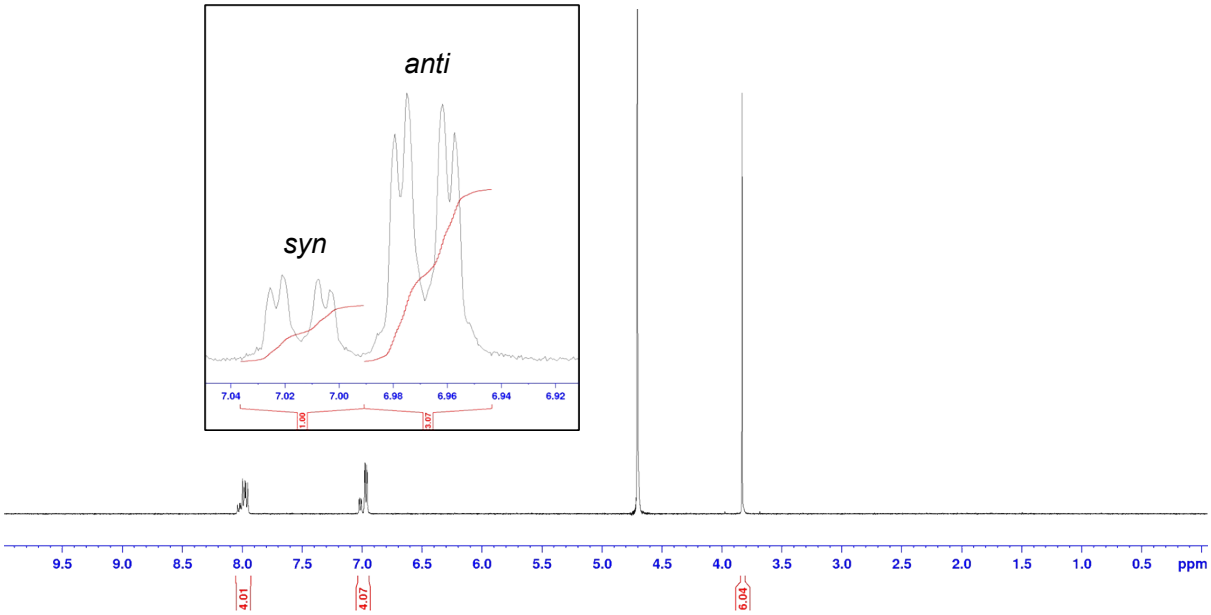

Figure S6. ^{1}H NMR of $(NH_4)_2[Pd(L_{PO})_2]$ recorded in D_2O at room temperature. Inset: *syn* and *anti*-distribution in solution.

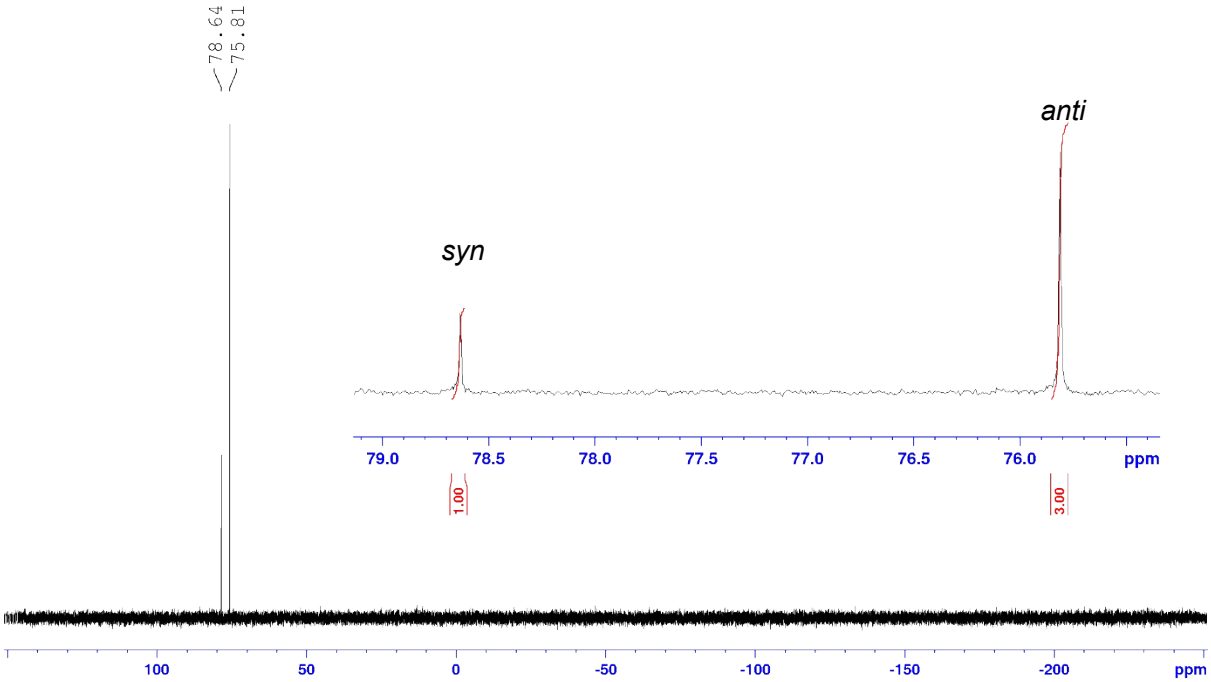

Figure S7. ^{31}P NMR of $(NH_4)_2[Pd(L_{PO})_2]$ recorded in D_2O at room temperature.

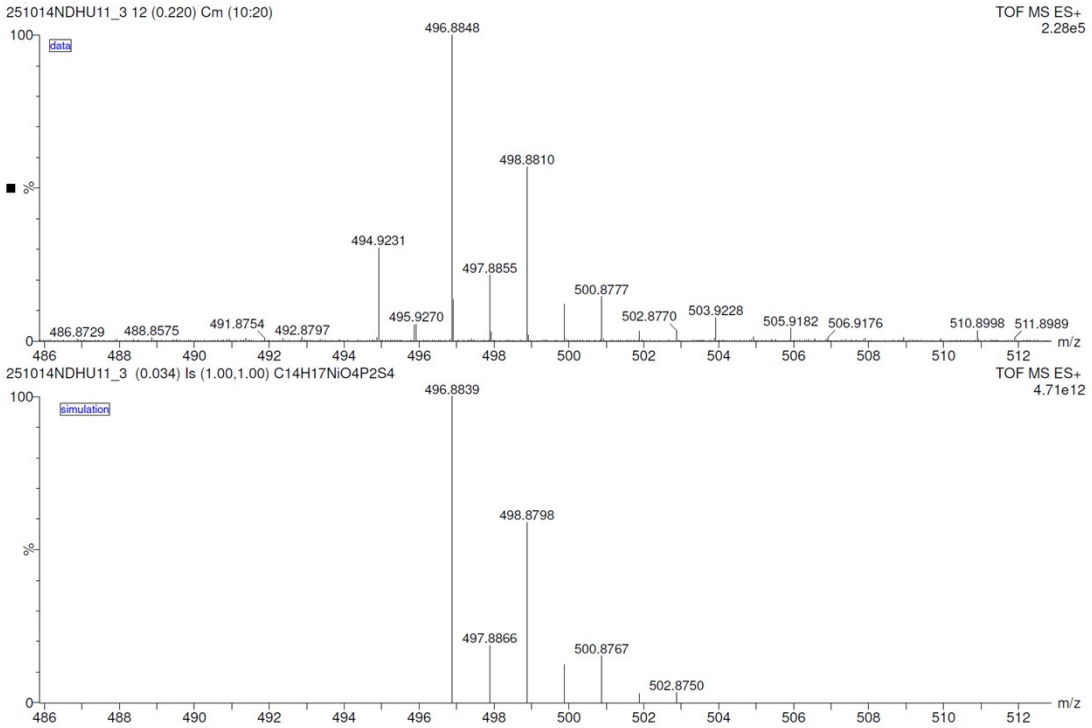

Figure S8. ESI-MS for $[Ni(L_{PO})_2 + 3H]^+$.

References

S1. W. E. Van Zyl and J. P. Fackler, *Phosphorus, Sulfur, Silicon Relat. Elem.*, 2000, **167**, 117–132.

S2. O. V. Dolomanov, L. J. Bourhis, R. J. Gildea, J. A. K. Howard and H. Puschmann, *J. Appl. Crystallogr.*, 2009, **42**, 339–341.

S3. L. J. Bourhis, O. V. Dolomanov, R. J. Gildea, J. A. K. Howard and H. Puschmann, *Acta Crystallogr. A.*, 2015, **71**, 59–75.

S4. Z. L. Xue, A. J. Ramirez-Cuesta, C. M. Brown, S. Calder, H. B. Cao, B. C. Chakoumakos, L. L. Daemen, A. Huq, A. I. Kolesnikov, E. Mamontov, A. A. Podlesnyak and X. P. Wang, *Eur. J. Inorg. Chem.*, 2019, **8**, 1065–1089.

S5. J. Zikovsky, P. Peterson, X. Wang, M. Frost and C. Hoffmann, *J. Appl. Crystallogr.*, 2011, **44**, 418–423.

S6. A. J. Schultz, M. Jorgensen, X. Wang, R. Mikkelson, D. Mikkelson, V. Lynch, P. Peterson, M. Green and C. Hoffmann, *J. Appl. Crystallogr.*, 2014, **47**, 915–921.

S7. A. J. Schultz, K. Srinivasan, R. G. Teller, J. M. Williams and C. M. Lukehart, *J. Am. Chem. Soc.*, 1984, **106**, 999–1003.

S8. Gaussian 16, Revision C.01, M. J. Frisch, G. W. Trucks, H. B. Schlegel, G. E. Scuseria, M. A. Robb, J. R. Cheeseman, G. Scalmani, V. Barone, G. A. Petersson, H. Nakatsuji, X. Li, M. Caricato, A. V. Marenich, J. Bloino, B. G. Janesko, R. Gomperts, B. Mennucci, H. P. Hratchian, J. V. Ortiz, A. F. Izmaylov, J. L. Sonnenberg, D. Williams-Young, F. Ding, F. Lipparini, F. Egidi, J. Goings, B. Peng, A. Petrone, T. Henderson, D. Ranasinghe, V. G. Zakrzewski, J. Gao, N. Rega, G. Zheng, W. Liang, M. Hada, M. Ehara, K. Toyota, R. Fukuda, J. Hasegawa, M. Ishida, T. Nakajima, Y. Honda, O. Kitao, H. Nakai, T. Vreven, K. Throssell, J. A. Montgomery, Jr., J. E. Peralta, F. Ogliaro, M. J. Bearpark, J. J. Heyd, E. N. Brothers, K. N. Kudin, V. N. Staroverov, T. A. Keith, R. Kobayashi, J. Normand, K. Raghavachari, A. P. Rendell, J. C. Burant, S. S. Iyengar, J. Tomasi, M. Cossi, J. M. Millam, M. Klene, C. Adamo, R. Cammi, J. W. Ochterski, R. L. Martin, K. Morokuma, O. Farkas, J. B. Foresman and D. J. Fox. Gaussian, Inc., Wallingford CT, 2016.

S9. A. D. Becke, *Phys. Rev. A*, 1988, **38**, 3098–3100.

S10. J. P. Perdew, *Phys. Rev. B*, 1986, **33**, 8822–8824.

S11. A. Schaefer, H. Horn and R. J. Ahlrichs, *J. Chem. Phys.*, 1992, **97**, 2571–2577.

S12. T. Yanai, D. Tew and N. Handy, *Chem. Phys. Lett.*, 2004, **393**, 51–57.